CAP-TSD: A PROGRAM FOR UNSTEADY TRANSONIC ANALYSIS OF REALISTIC AIRCRAFT CONFIGURATIONS

John T. Batina
David A. Seidel
Samuel R. Bland
Robert M. Bennett
Unsteady Aerodynamics Branch
NASA Langley Research Center
Hampton, Virginia

PRECEDING PAGE BLANK NOT FILMED

OVERVIEW

The presentation describes the development of a new transonic code to predict unsteady flows about realistic aircraft configurations. The work has been a major research activity over the past year within the Unsteady Aerodynamics Branch at NASA Langley Research Center. The presentation first describes an approximate factorization algorithm for solution of the unsteady transonic small-disturbance (TSD) equation. Because of the superior stability characteristics of the AF algorithm, a new transonic aeroelasticity code has been developed which is described in some detail. The new code was very easy to modify to include the additional aircraft components, so in a very short period of time the code has been developed to treat complete aircraft configurations. Finally, applications are presented which demonstrate many of the geometry capabilities of the new code.

- Describe Approximate Factorization (AF) algorithm
- Demonstrate superior stability characteristics of AF algorithm
- Introduce new transonic aeroelasticity code
- Describe complete aircraft modeling
- Applications

APPROXIMATE FACTORIZATION ALGORITHM DEVELOPED

A new algorithm based on approximate factorization (AF) was recently developed by Batina (Ref. 1) for the time-accurate solution of the unsteady TSD equation. The AF algorithm involves a Newton linearization procedure coupled with an internal iteration technique. In Ref. 1 the AF algorithm was shown to be very robust and efficient for application to either steady or oscillatory transonic flows with subsonic or supersonic freestream conditions. The new algorithm can provide accurate solutions in only several hundred time steps yielding a significant computational cost savings when compared to alternative methods. Furthermore, the AF algorithm is fully vectorizable which results in an additional saving of computer resources.

- Time-accurate solution of TSD equation
- Involves Newton linearization coupled with internal iterations
- Stable for relatively large time steps
- Fully implicit and vectorizable in all three coordinate directions
- Enables supersonic freestream calculations

APPROXIMATE FACTORIZATION ALGORITHM OVERVIEW

Shown here is a brief overview of the AF algorithm. A much more detailed description is given in Ref. 1. Basically, if the TSD equation is written in general form as $R(\phi^{n+1}) = 0$, then the solution is given by iteration of the Newton linearization. In this equation, $\Delta\phi$ is equal to $\phi^{n+1} - \phi^*$ where ϕ^* is the currently available value of ϕ^{n+1}. During convergence of the iteration procedure, $\Delta\phi$ is driven to zero so the solution is given by ϕ^*. The equation is solved numerically by approximately factoring $\partial R/\partial\phi$ into a triple product of operators and then sequentially applying the operators using three sweeps through the grid.

- TSD equation general form

$$R(\phi^{n+1}) = 0$$

- Solution by Newton linearization and internal iteration

$$R(\phi^*) + \left(\frac{\partial R}{\partial \phi}\right)_{\phi = \phi^*} \Delta\phi = 0$$

$$\text{where } \Delta\phi = \phi^{n+1} - \phi^*$$

- AF Algorithm

$$L_\xi L_\eta L_\zeta \Delta\phi = -R(\phi^*)$$

$$\text{where } L_\xi L_\eta L_\zeta \approx \left(\frac{\partial R}{\partial \phi}\right)_{\phi = \phi^*}$$

CONVERGENCE STUDY FOR UNSTEADY APPLICATIONS

With the AF algorithm, the step size may now be selected based on accuracy, rather than on numerical stability. To demonstrate this, a convergence study was performed for the F-5 wing at M = 0.9, to determine the largest step size that would produce converged results. Unsteady results were obtained using 100, 200, 300, and 400 steps per cycle of motion which required Δt = 0.2293, 0.1147, 0.0764, and 0.0573, respectively. The calculation for 100 steps per cycle produced reasonable results but fairly large differences were observed with the 200 steps per cycle calculation. As shown in this figure, the results for 200 and 300 steps per cycle are very similar, although there are small differences near the leading edge and in the shock pulse region. The results for 400 steps per cycle are essentially the same as those for 300. Therefore, it takes about 300 steps per cycle to produce converged results, although the results for 200 steps per cycle may be acceptable for engineering purposes.

- F-5 wing upper surface pressures for rigid pitching at M = 0.9 and k = 0.137

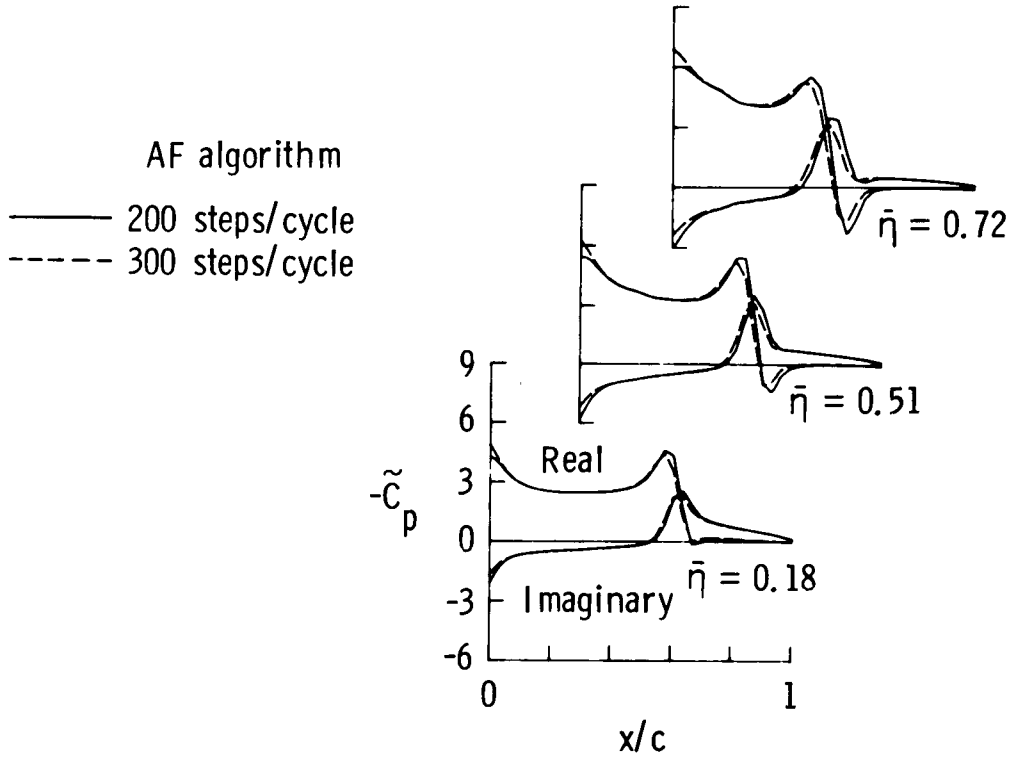

CAP-TSD: COMPUTATIONAL AEROELASTICITY PROGRAM - TRANSONIC SMALL DISTURBANCE

Because of the superior stability characteristics and computational efficiency of the AF algorithm, a new transonic code has been developed for aeroelastic applications. The new code is called CAP-TSD (Ref. 2) which is an acronym for Computational Aeroelasticity Program - Transonic Small Disturbance. As the name implies, the code solves the unsteady transonic small-disturbance equation based on the AF algorithm. The purpose of the CAP-TSD code is for static and dynamic aeroelastic applications. The code is highly vectorized and thus is very fast. In comparison with XTRAN3S, for example, CAP-TSD is about six times faster on a per time step basis. Also, the code is capable of treating complete aircraft configurations.

- Based on approximate factorization algorithm
- Static and dynamic aeroelastic applications
- Code is highly vectorized: very fast

XTRAN3S V1.5	CAP - TSD
0.62 CPU SEC/Δt	0.1 CPU SEC/Δt

- Computational expense $\sim N\left(=\frac{T}{\Delta t}\right) \times$ CPU SEC/Δt

  Potential savings factor $\sim 20 \times 6 \geq 100$

- Capable of treating complete aircraft configurations

COMPLETE AIRCRAFT MODELING WITH CAP-TSD

This includes multiple lifting surfaces, the fuselage, pylons/stores/nacelles, as well as leading and trailing edge control surfaces. Furthermore, these components may be arbitrarily placed within the computational domain to allow for a full-span modeling capability. With this capability, one can then treat antisymmetric mode shapes or unsymmetric geometries such as an oblique wing or even unsymmetric store configurations.

- Multiple lifting surfaces (canard/wing/tail)
- Fuselage
- Pylons/stores/nacelles
- Leading and trailing edge control surfaces
- Components may be arbitrarily placed within computational domain
  - Full span capability
  - Antisymmetric mode shapes or unsymmetric geometries allowed

COMPLETE AIRCRAFT MODELING WITH CAP-TSD

Shown here are several of the complex configurations that have been modeled using CAP-TSD. The figure illustrates how combinations of lifting surfaces and bodies are used to model realistic geometries.

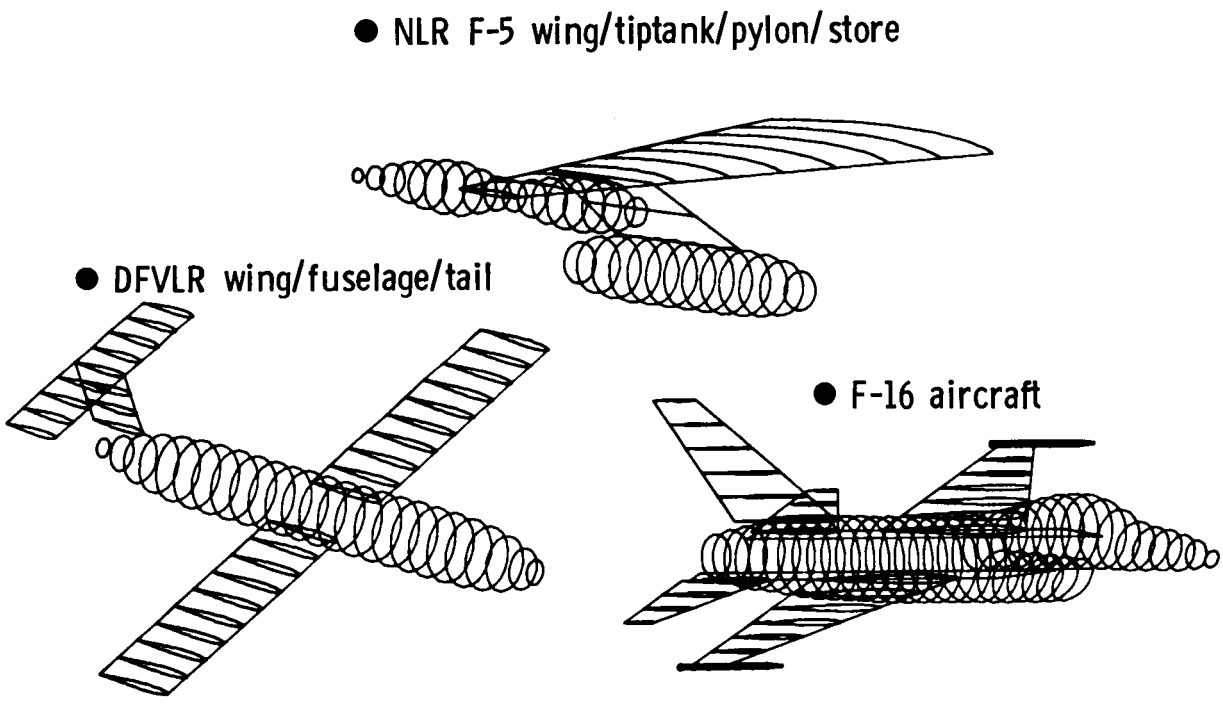

CONFIGURATIONS ANALYZED USING CAP-TSD

Results are presented next for the five configurations shown here, which demonstrate many of the CAP-TSD geometry capabilities. These configurations range in geometrical complexity from a simple wing with control surface to a realistic fighter geometry. The five configurations were selected to assess various geometry capabilities of CAP-TSD by making comparisons with the experimental pressure data of Refs. 3-9. The configurations include: The F-5 wing with an inboard trailing edge control surface (Ref. 3); the F-5 wing with an area-ruled tiptank and underwing pylon/store (Refs. 4 and 5); a simple wing/fuselage/tail configuration that was tested at the DFVLR (Ref. 6); a canard/wing/fuselage model tested by Rockwell (Ref. 7); and finally, the General Dynamics one-ninth scale F-16C aircraft model (Ref. 8).

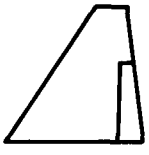

F-5 wing/
control surface

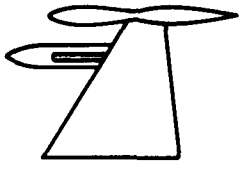

F-5 wing/tiptank/
pylon/store

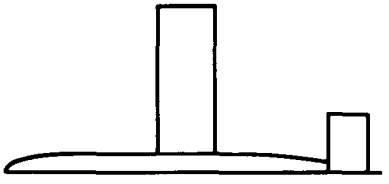

DFVLR wing/
fuselage/tail

Rockwell canard/
wing/fuselage

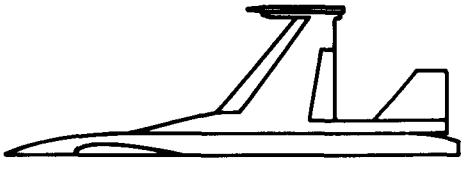

General Dynamics
F-16C aircraft model

RESULTS FOR F-5 WING/CONTROL SURFACE CONFIGURATION

Results were obtained for the F-5 wing/control surface configuration to assess the accuracy and efficiency of the CAP-TSD code for oscillatory control surface applications. The wing has a panel aspect ratio of 1.58, a leading edge sweep angle of 31.9°, and a taper ratio of 0.28. The airfoil section of the F-5 wing is a modified NACA 65A004.8 airfoil which has a drooped nose and is symmetric aft of 40% chord. The control surface has a constant-percent-chord hinge line at 82% chord, inboard side edge at the wing root, and outboard side edge at 58% semispan. The calculations are compared with the experimental oscillatory pressure data from an F-5 wing model tested by Persoon, Roos, and Schippers (Ref. 3). Both subsonic and supersonic freestream cases are presented. Steady pressure distributions for these cases were presented and compared with the experimental data in Ref. 1, and therefore are not repeated here. Unsteady pressure results are described as follows.

- Case 1: M = 0.9, unsteady flow
- Case 2: M = 1.1, unsteady flow

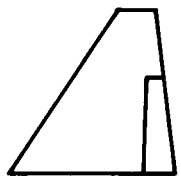

F-5 wing/
control surface

F-5 WING/OSCILLATING CONTROL SURFACE APPLICATION

At the subsonic freestream Mach number of 0.9, unsteady results were obtained for the control surface oscillating with an amplitude of 0.471° at a reduced frequency of 0.139. The calculations were performed using only 300 steps per cycle of motion which corresponds to a step size of $\Delta t = 0.07354$. Three cycles of motion were computed to obtain a periodic solution. Unsteady pressure distributions along three chords of the wing are shown in this figure along with the experimental data. These pressures are plotted as real and imaginary components corresponding to the in-phase and out-of-phase unsteady pressure distributions normalized by the amplitude of motion. The CAP-TSD results agree well with the data, especially in predicting the control surface pressures and the hinge-line singularity at 82% chord.

- Lower surface unsteady pressures at $\delta_1 = 0.471°$ and $k = 0.139$

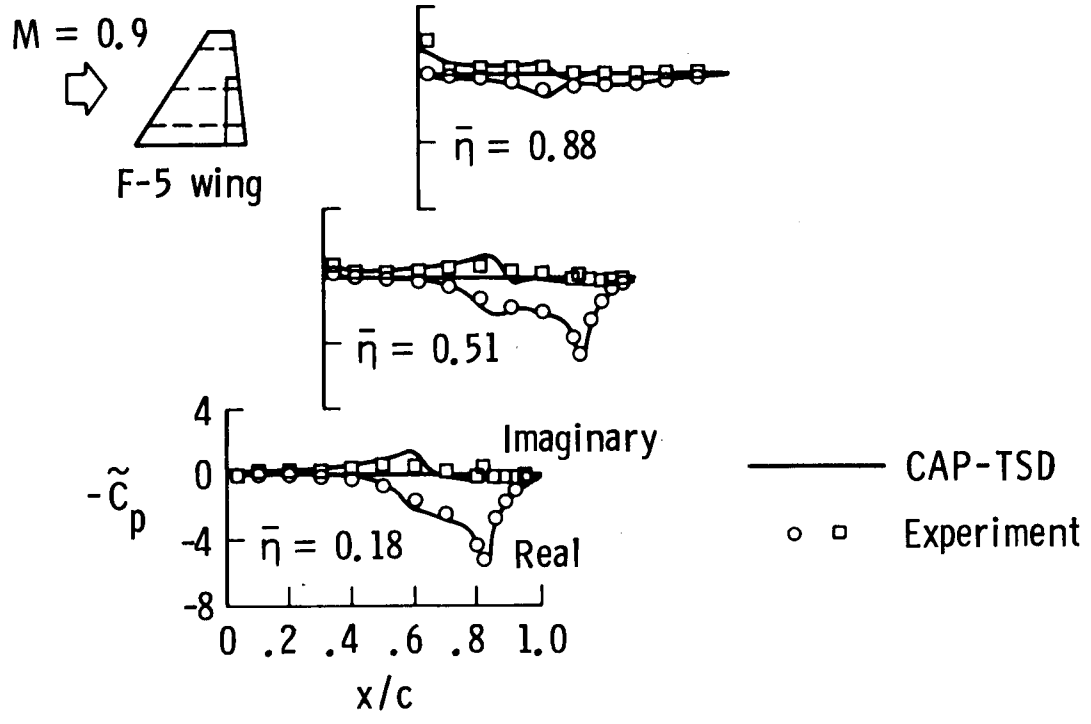

F-5 WING/OSCILLATING CONTROL SURFACE APPLICATION

At the supersonic freestream Mach number of 1.1, the unsteady results were obtained for the control surface oscillating with an amplitude of 0.45° at a reduced frequency of 0.118. These calculations were also performed using only 300 steps per cycle of motion which corresponds to a step size of $\Delta t = 0.08875$. Only two cycles of motion were required to obtain a periodic solution. Calculations for the third cycle of motion produced results that were identical to the second cycle results, to plotting accuracy. This faster convergence is due to the lack of upstream signal propagation resulting from the supersonic nature of the flow. The results indicate that the pressures on the control surface are nearly in-phase with the motion since the imaginary components are very small in comparison with the real components. Also, the pressures are zero outside of the domain of influence of the control surface which is expected for supersonic flow. The CAP-TSD results are in very good agreement with the experimental data. Further applications of CAP-TSD including comparisons with experiment for supersonic freestream cases are reported in Ref. 10.

- Upper surface unsteady pressures at $\delta_1 = 0.45°$ and $k = 0.118$

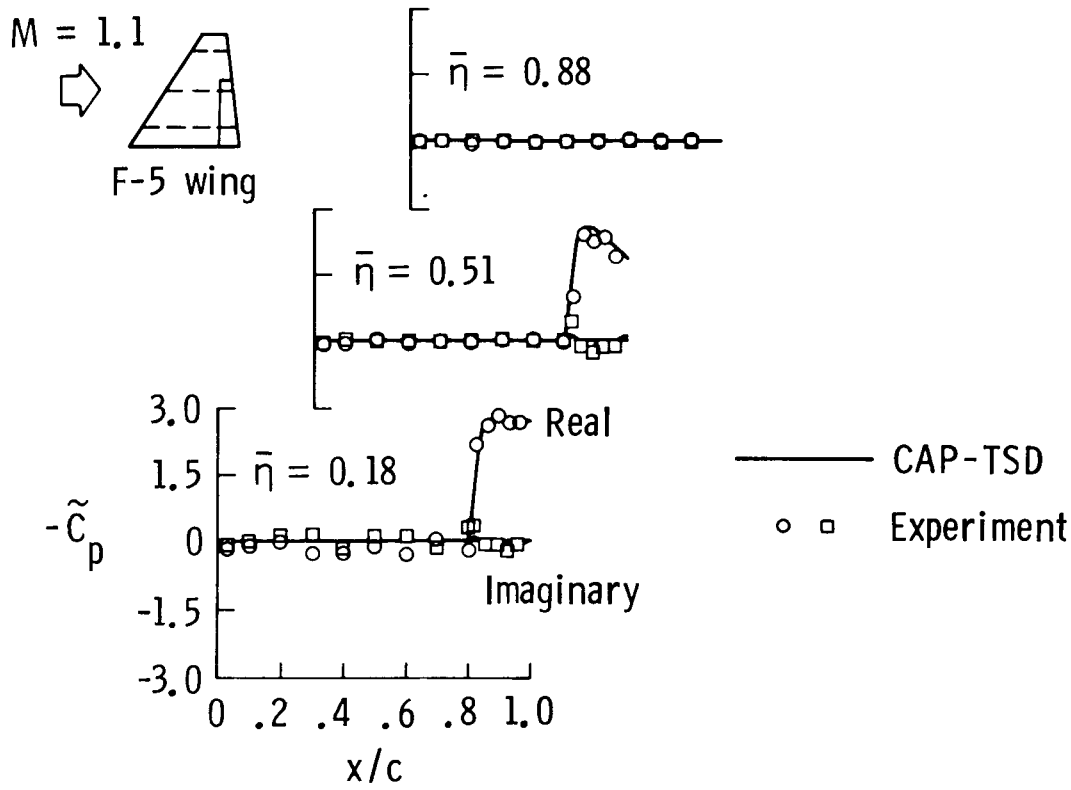

RESULTS FOR
F-5 WING/TIPTANK/PYLON/STORE CONFIGURATION

Results were next obtained for the F-5 wing with tiptank and pylon/store to assess CAP-TSD for multiple body geometries. For this configuration, three components have been modeled in addition to the F-5 wing: (1) an area-ruled tiptank which is an axisymmetric body of revolution with a fineness ratio (length/maximum diameter) of 10.88; (2) an underwing store which is also an axisymmetric body of revolution with a fineness ratio of 7.04; and (3) a pylon which connects the store to the lower surface of the wing at 77% semispan. The tiptank and store have angles of incidence relative to the wing zero angle of attack of -2.0° and -2.5°, respectively. A more detailed description of the F-5 wing/tiptank/pylon/store configuration is given in Refs. 4 and 5 along with the experimental pressure data. The calculations were performed for combinations of F-5 components to investigate aerodynamic interference effects on steady and unsteady wing pressures. In these calculations the freestream Mach number was selected as 0.45 for comparison with the subsonic data published by the NLR.

- Case 3: M = 0.45, steady and unsteady flows

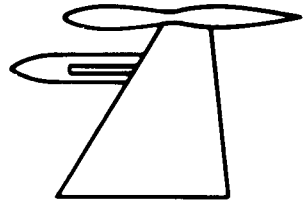

F-5 wing/tiptank/
pylon/store

F-5 TIPTANK STEADY PRESSURE COMPARISONS

For this case, steady pressure distributions are presented first for the tiptank, to assess the accuracy of the body modeling. Two sets of pressures are plotted corresponding to inboard (θ = 157.5°) and outboard (θ = 22.5°) longitudinal lines along the tiptank. These pressure distributions show expansions near the fore and aft maximum diameter locations and a compression near the area-ruled middle region. The calculated tiptank pressures are in good agreement with the experimental data.

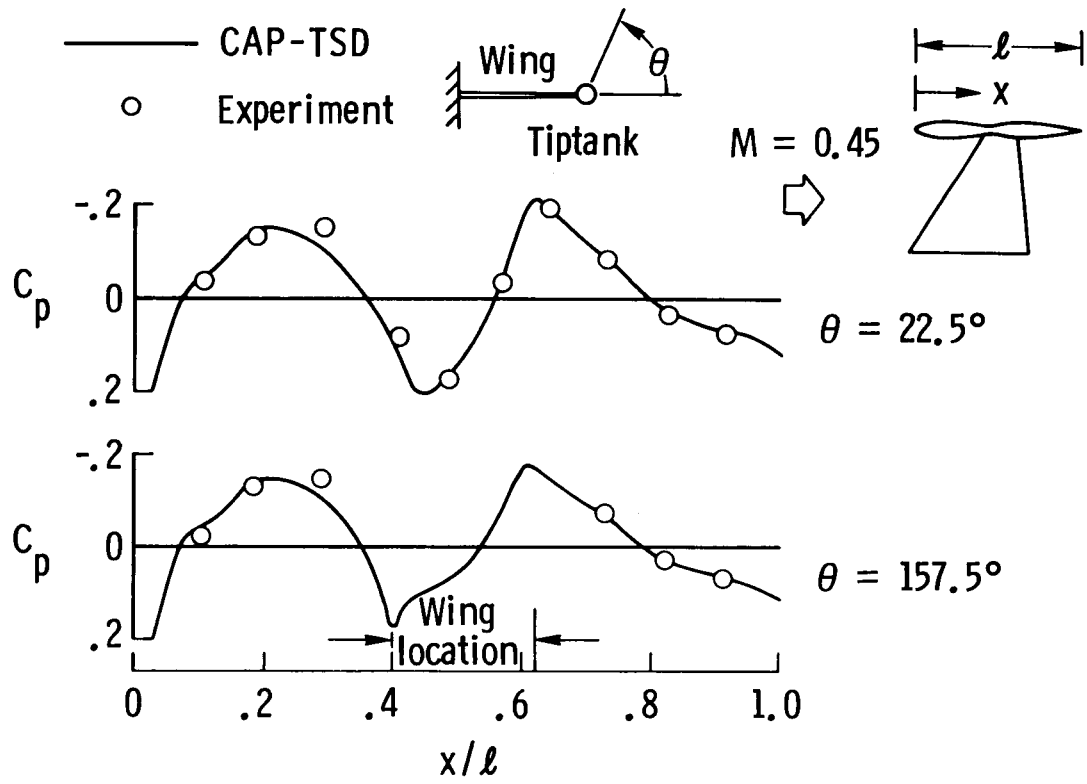

EFFECT OF PYLON/STORE ON STEADY PRESSURES

Steady pressure distributions on the wing are presented here for the 72% semispan station. Two sets of calculated and experimental results are plotted corresponding to the wing/tiptank configuration with and without the pylon/store. As shown in the lower part of the figure, inclusion of the pylon and store significantly increased the lower surface pressures from the wing leading edge to approximately 60% chord. The effect of the pylon/store on the upper surface pressures is negligible, as shown in the upper part of the figure. The calculated steady pressures for cases with and without the pylon/store compare well with the experimental data.

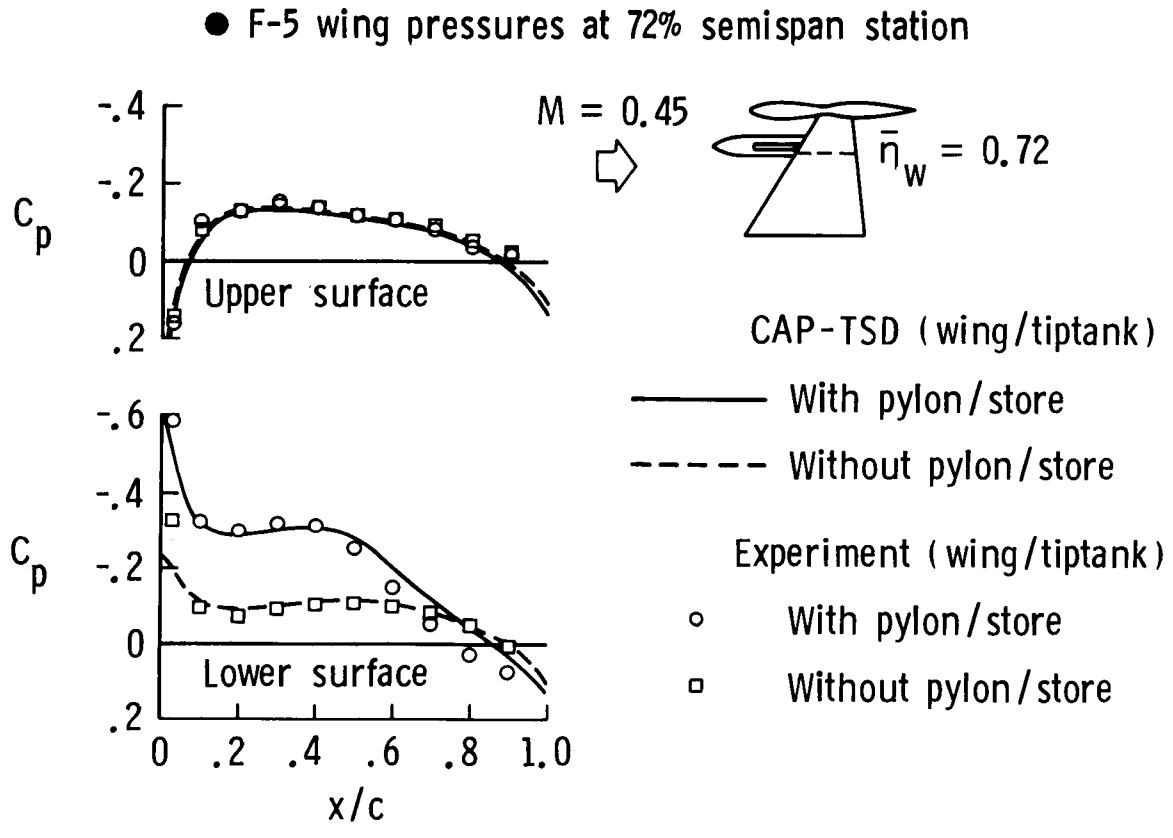

EFFECT OF PYLON/STORE ON UNSTEADY PRESSURES

This figure shows the effect of the pylon/store on the unsteady pressure distributions. The unsteady calculations were performed for the configuration pitching harmonically at a reduced frequency of k = 0.147. The configuration was forced to pitch about a line perpendicular to the root at 15% chord from the wing apex. The results were obtained using 300 steps per cycle of motion which corresponds to a step size of $\Delta t = 0.07135$. Two sets of results are again presented corresponding to the wing/tiptank configuration with and without the pylon/store. As shown in the upper part of the figure, inclusion of the pylon and store increased the real component of the unsteady lifting pressure, similar to the steady-state interference effect. The effect on the imaginary part is negligible. The CAP-TSD results are again in good agreement with the experimental pressure data in predicting the aerodynamic interference effects of the pylon/store.

- F-5 configuration pitching about 15% root chord at k = 0.147

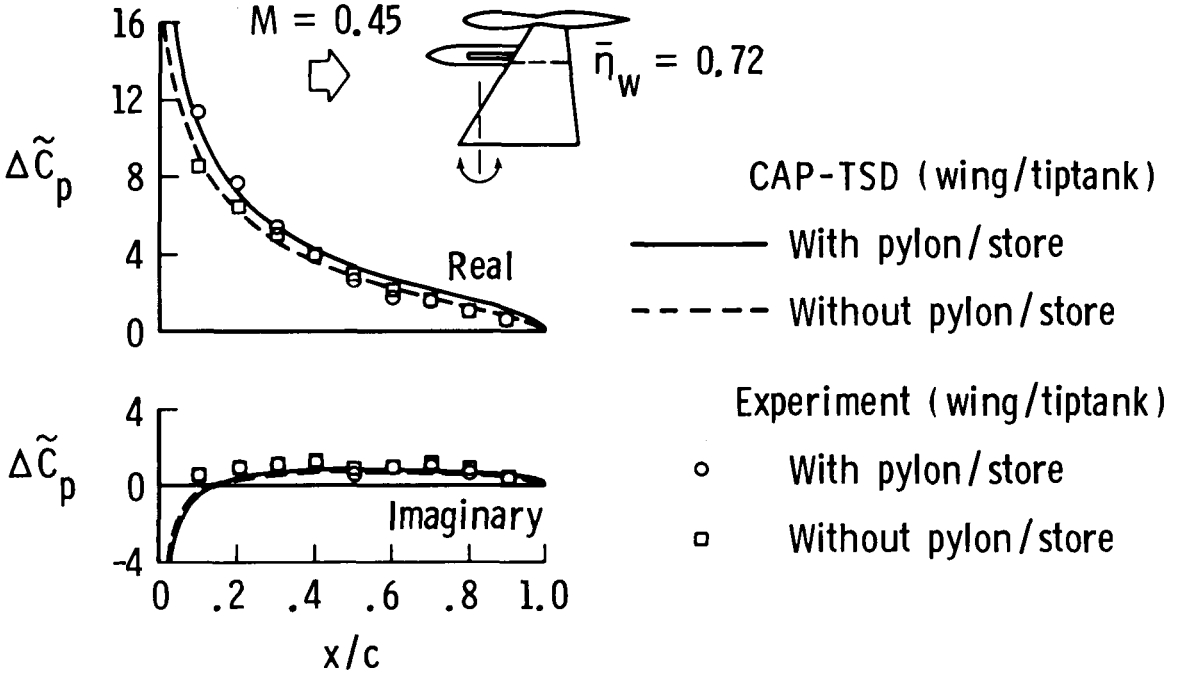

RESULTS FOR
DFVLR WING/FUSELAGE/TAIL CONFIGURATION

For the DFVLR wing/fuselage/tail configuration, results were obtained to assess the accuracy of CAP-TSD for multiple lifting surface and fuselage applications. The DFVLR configuration consists of a rectangular-planform wing that is centrally mounted to a circular cross-section fuselage with a T-tail. The wing has a panel (exposed) aspect ratio of 2.66 and an RAE 101 airfoil section (9% maximum thickness-to-chord ratio). The axisymmetric fuselage has a fineness ratio of 9.75. The horizontal tail has a panel aspect ratio of 1.5 and an RAE 101 airfoil section (12.7% maximum thickness-to-chord ratio). It is located above the wing mean plane, a distance equal to the fuselage maximum diameter, and is connected to the fuselage by the rectangular vertical tail. The DFVLR wing/fuselage/tail configuration is further described in Ref. 6 along with the low-speed experimental steady pressure data. In these calculations, the freestream Mach number was selected as 0.2 for comparison with the data. For this case as well as for the remaining complex configurations, only steady-state comparisons with experiment are given. This is because, in general, there is a lack of experimental unsteady pressure data on complex configurations to validate time-accurate computer codes.

- Case 4: M = 0.2, steady flow

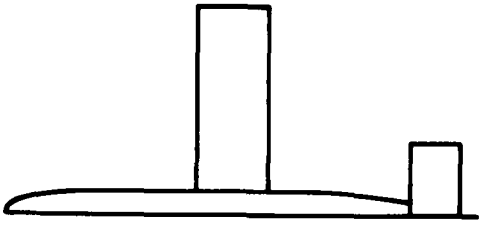

DFVLR wing/
fuselage/tail

DFVLR CONFIGURATION STEADY PRESSURE COMPARISON

For the DFVLR configuration, comparisons of CAP-TSD and experimental steady pressures on the upper surfaces of the wing and tail are shown in the figure. Chordwise pressures along three span stations of the wing and along one span station of the tail were selected for comparison with the data. The angle of attack of the wing was 0.25°. The angle of attack for the tail and fuselage was 0.15°. The CAP-TSD results compare very well with the data along both lifting surfaces except in the vicinity of the wing leading edge.

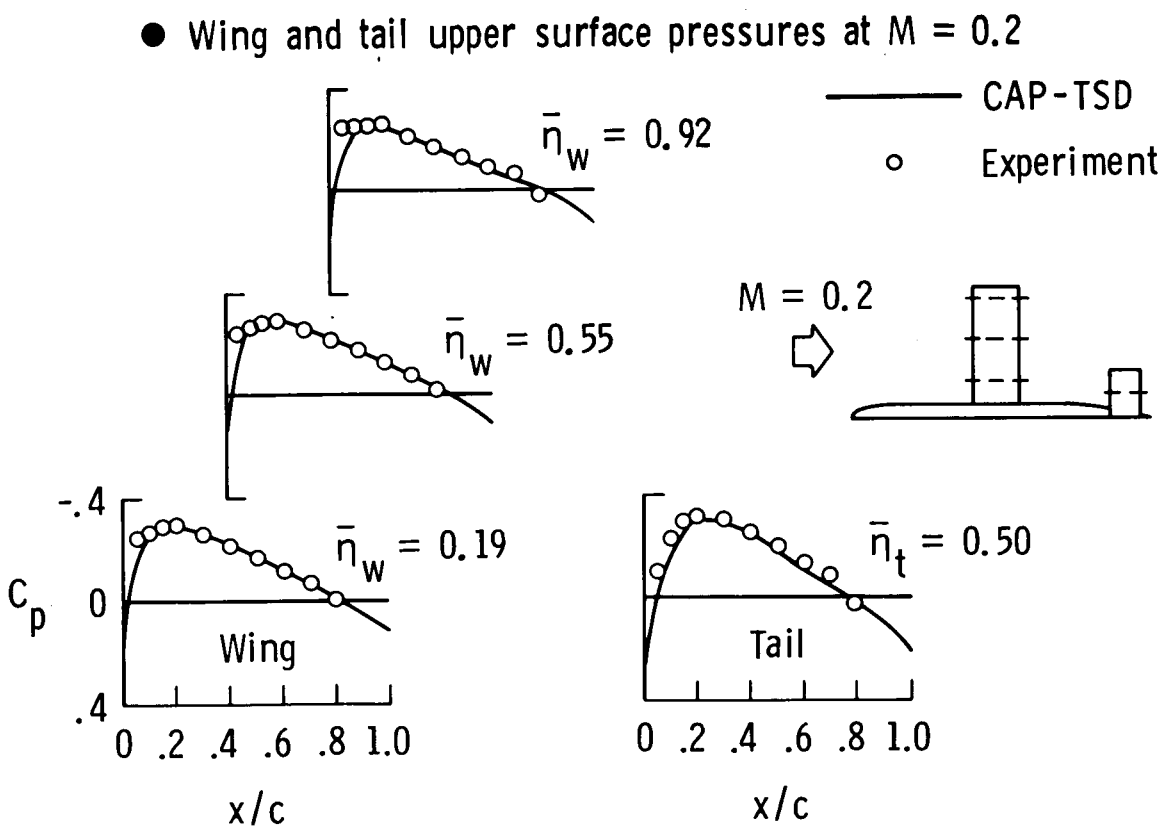

DFVLR CONFIGURATION STEADY PRESSURE COMPARISON FOR FUSELAGE

This figure shows similar comparisons between CAP-TSD and experiment for the fuselage of the DFVLR configuration. Two sets of longitudinal pressures are plotted corresponding to the fuselage upper centerline ($\theta = 90°$) and to a line that passes close to the wing-fuselage junction ($\theta = 20°$). The calculated pressures are again in good agreement with the experimental data even in the critical wing-fuselage junction region. This good agreement thus validates the CAP-TSD code for application to multiple-component configurations such as the DFVLR wing/fuselage/tail.

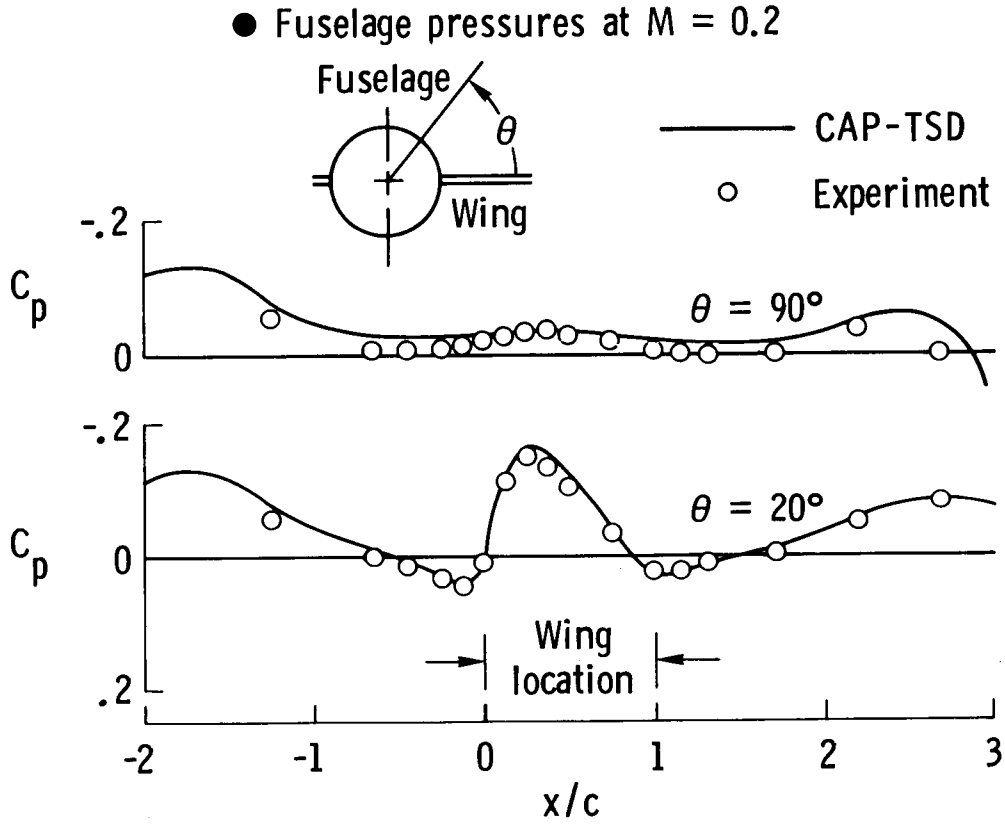

RESULTS FOR
ROCKWELL CANARD/WING/FUSELAGE CONFIGURATION

To further assess CAP-TSD for multiple lifting surface and fuselage applications, results were obtained for the Rockwell canard/wing/fuselage configuration. This configuration consists of a swept-tapered canard and wing mounted to a relatively simple half-span fuselage. Each of the non-coplanar lifting surfaces has a panel (exposed) aspect ratio of approximately 1.0, a leading edge sweep angle of 40°, a taper ratio slightly greater than 0.25, and a supercritical airfoil section. The wing also has 4° of incidence relative to the fuselage and 5° of parabolic twist washout. The Rockwell canard/wing/fuselage configuration is further described in Ref. 7 along with the experimental steady pressure data. In the CAP-TSD comparisons presented here, the freestream Mach number was 0.8.

- Case 5: M = 0.8, steady flow

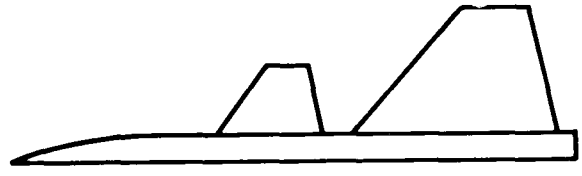

Rockwell canard/
wing/fuselage

ROCKWELL CONFIGURATION STEADY PRESSURE COMPARISON

For this case, the angle of attack for both the canard and the wing was 2.05°. For the wing, this angle is added to the incidence and twist so that the root and tip are effectively at 6.05° and 1.05°, respectively. The figure shows chordwise pressures along one span station of the canard and along three span stations of the wing. The CAP-TSD pressures are in favorable agreement with the experimental data along both lifting surfaces. The small differences between calculation and experiment in the wing upper surface trailing edge region, are due to flow separation. The overpredicted pressures along the lower surface of both the canard and the wing, aft of approximately 85% chord, are due to viscous effects. Of course, flow separation and viscous effects are outside the scope of the present capability.

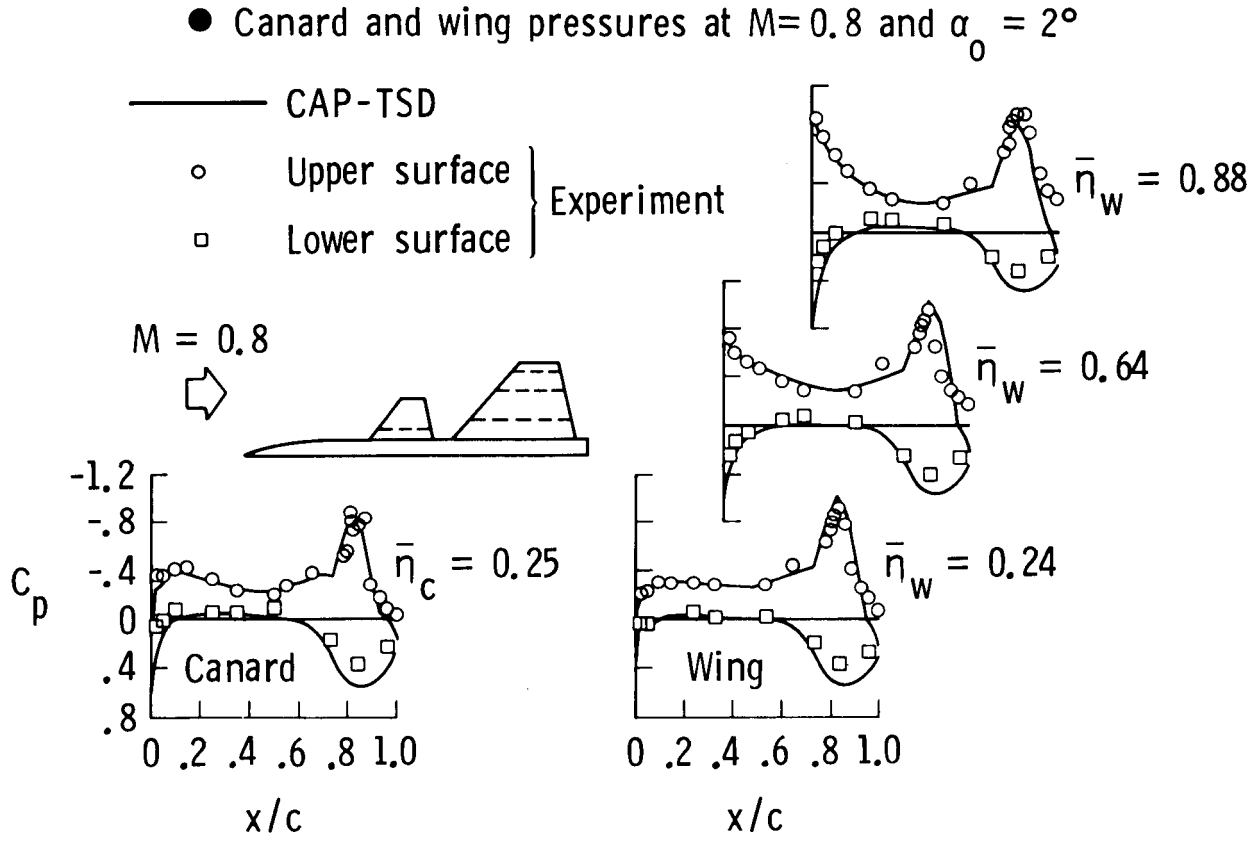

RESULTS FOR GENERAL DYNAMICS F-16C AIRCRAFT MODEL

Finally, results were obtained for the General Dynamics F-16C aircraft model to demonstrate application of CAP-TSD to a realistic configuration. The calculations were performed for three Mach numbers including 0.85, 0.9, and 1.1. In each case, CAP-TSD results were obtained for the F-16C aircraft at approximately 2.3° angle of attack and with the leading edge control surface of the wing deflected upwards 2° for comparison with the experimental steady pressure data of Ref. 9. These steady pressure comparisons were made to assess the accuracy of CAP-TSD for complete airplane applications. All of the results were originally reported in Ref. 1. The results presented here are for the M = 0.9 case.

- Case 6: M = 0.85, steady flow
- Case 7: M = 0.90, steady and unsteady flows
- Case 8: M = 1.10, steady flow

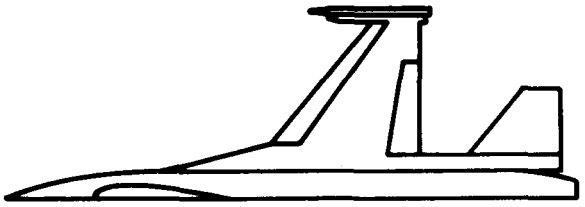

General Dynamics
F-16C aircraft model

CAP-TSD MODELING OF F-16C AIRCRAFT

In these calculations, the F-16C is modeled using four lifting surfaces and two bodies. The lifting surfaces include: (1) the wing with leading and trailing edge control surfaces; (2) the launcher; (3) a highly-swept strake, and shelf surface; and (4) the horizontal tail. The bodies include: (1) the tip missile and (2) the fuselage. Other salient features of the F-16C modeling include 3° linear twist washout for the wing, a leading edge control surface hinge line that is straight but not of constant-percent chord, and 10° anhedral for the horizontal tail. The rather detailed geometry description for the one-ninth scale F-16C aircraft model was obtained from Ref. 8 and the experimental steady pressure data is tabulated in Ref. 9. All of the calculations were performed on a cartesian grid that conforms to the leading and trailing edges of the lifting surfaces which contains 324,000 points. The grid was fairly easy to generate, even for a complex configuration such as the F-16, because it is cartesian.

There are no unsteady experimental data to validate the CAP-TSD code for time-accurate F-16C calculations. Nonetheless, an unsteady calculation was performed for the M = 0.9 case, to demonstrate the time-accurate capability. For simplicity, the calculation was performed for a rigid pitching motion where the entire F-16C aircraft was forced to oscillate about the model moment reference axis. Parallel calculations were also performed for the wing alone, to investigate the effects of aerodynamic interference by making comparisons with the complete airplane results. These wing-alone calculations were performed for the outer wing panel only, with a plane of symmetry assumed at the wing root.

- Modeled using four lifting surfaces and two bodies
- Cartesian grid with 324 000 points

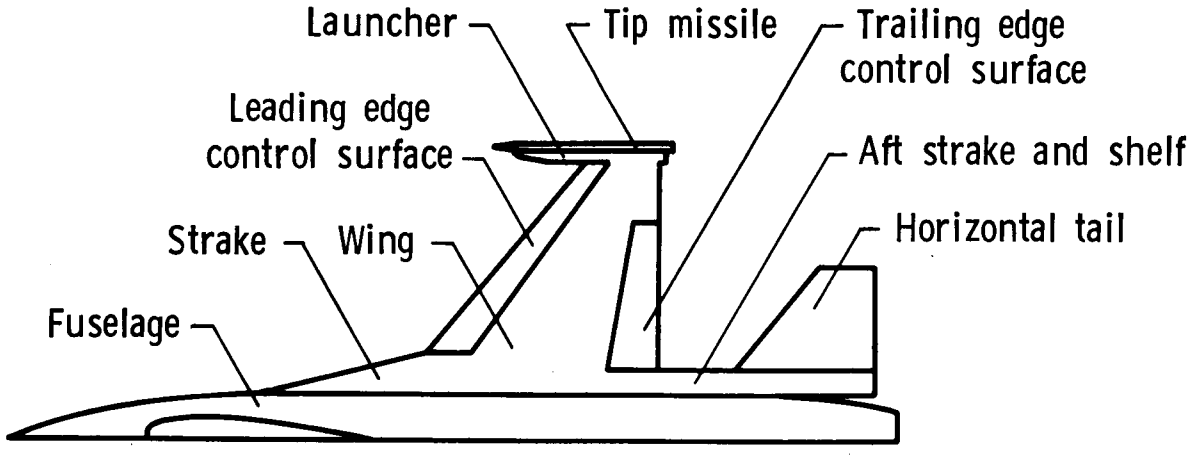

F-16C AIRCRAFT STEADY PRESSURE COMPARISON

Steady pressure comparisons are presented here for three span stations of the wing and one span station of the tail. For this case (M = 0.9), there is a moderately strong shock wave on the upper surface of the wing and the CAP-TSD pressures again generally agree well with the experimental pressures. The shock is slightly overpredicted in strength and located slightly aft of the experimental location which is expected from a conservative inviscid potential flow code. The inclusion of the nonisentropic effects (Ref. 11) and viscous effects (Ref. 12) could be expected to improve the correlation between calculation and experiment. For the tail, the flow is predominantly subcritical and the CAP-TSD pressures agree well with the experimental data. Also, the calculations required only 0.88 CPU seconds per time step on the VPS-32 computer at NASA Langley Research Center.

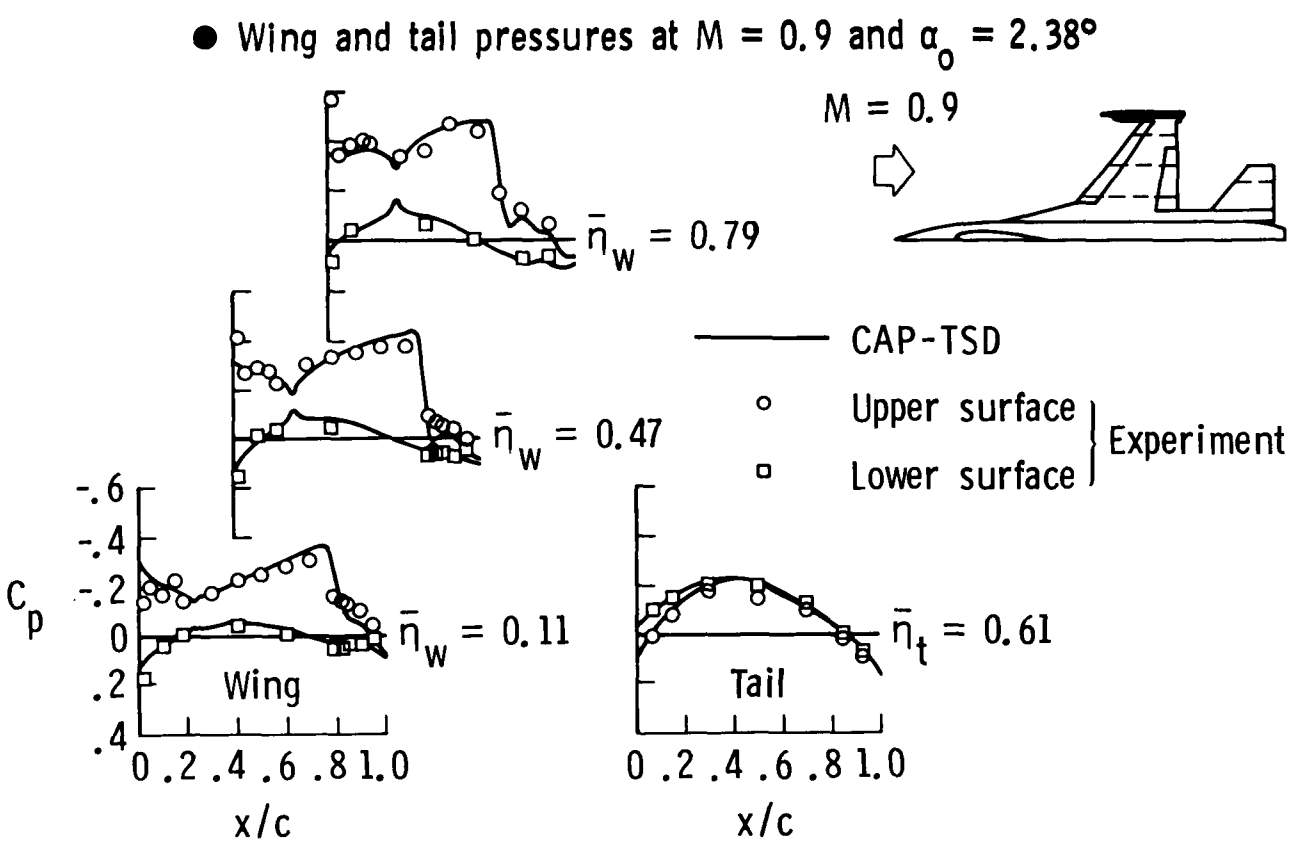

F-16C AIRCRAFT UNSTEADY PRESSURE COMPARISON

This figure shows the unsteady pressures for the entire F-16C aircraft undergoing a rigid pitching oscillation. Two sets of calculated pressures are compared, corresponding to complete airplane and wing alone modeling. The reduced frequency was selected as 0.1, the oscillation amplitude was chosen as $\alpha_1 = 0.5^o$, and 300 steps per cycle of motion were used. As shown in the figure, there is a relatively large shock pulse in the real part of the wing upper surface pressures. This shock pulse is of larger magnitude and is located further downstream in the complete airplane model. These features are attributed to a stronger steady-state shock on the upper surface of the wing produced by the accelerated flow about the fuselage and the launcher/tip missile. The unsteady pressures near the leading edge of the wing are also generally of larger magnitude for the complete airplane. For the tail, the unsteady pressures are relatively small in comparison with the wing pressures and thus were plotted on an expanded scale. The tail is located considerably aft of the pitch axis and thus its motion is plunge dominated which results in smaller airloads for the low value of k considered. Furthermore, these pressures are nearly 90° out of phase with the aircraft motion since the real components are small compared to the imaginary components. Also, the differences between complete airplane and wing-alone results emphasize the importance of including all of the aircraft components in the calculation.

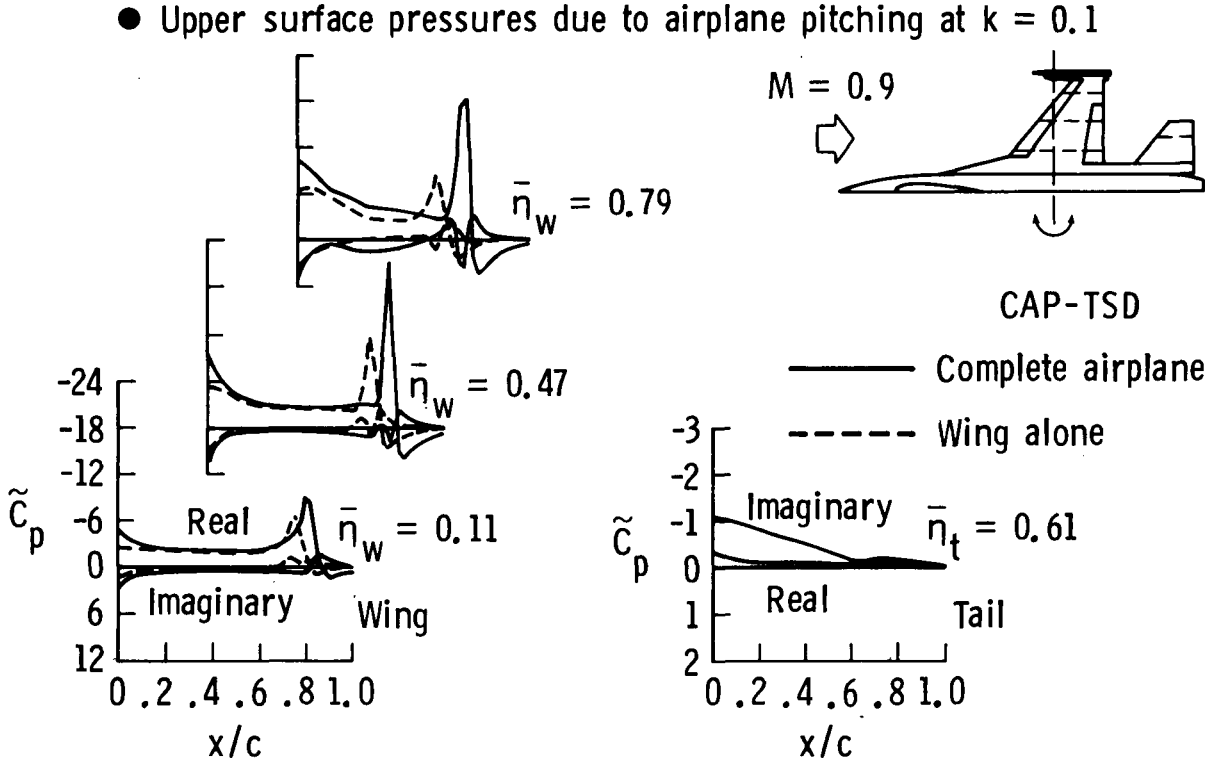

STEADY FLOW FIELD PRESSURES FOR F-16C AIRCRAFT

The following sequence of figures shows steady and unsteady pressure contours for the F-16C aircraft. The view shown in the first set of figures is an oblique projection of the aircraft. In this view, contours are plotted in vertical planes at four span stations along each wing as well as along the vehicle centerline. This figure shows the steady flow field pressures at M = 0.9 and $\alpha_0 = 2.38^0$. The contours indicate that there is flow compression along the leading and trailing edges of the wing and forward along the canopy. Flow expansion is indicated above the wing and fuselage, and above the canopy.

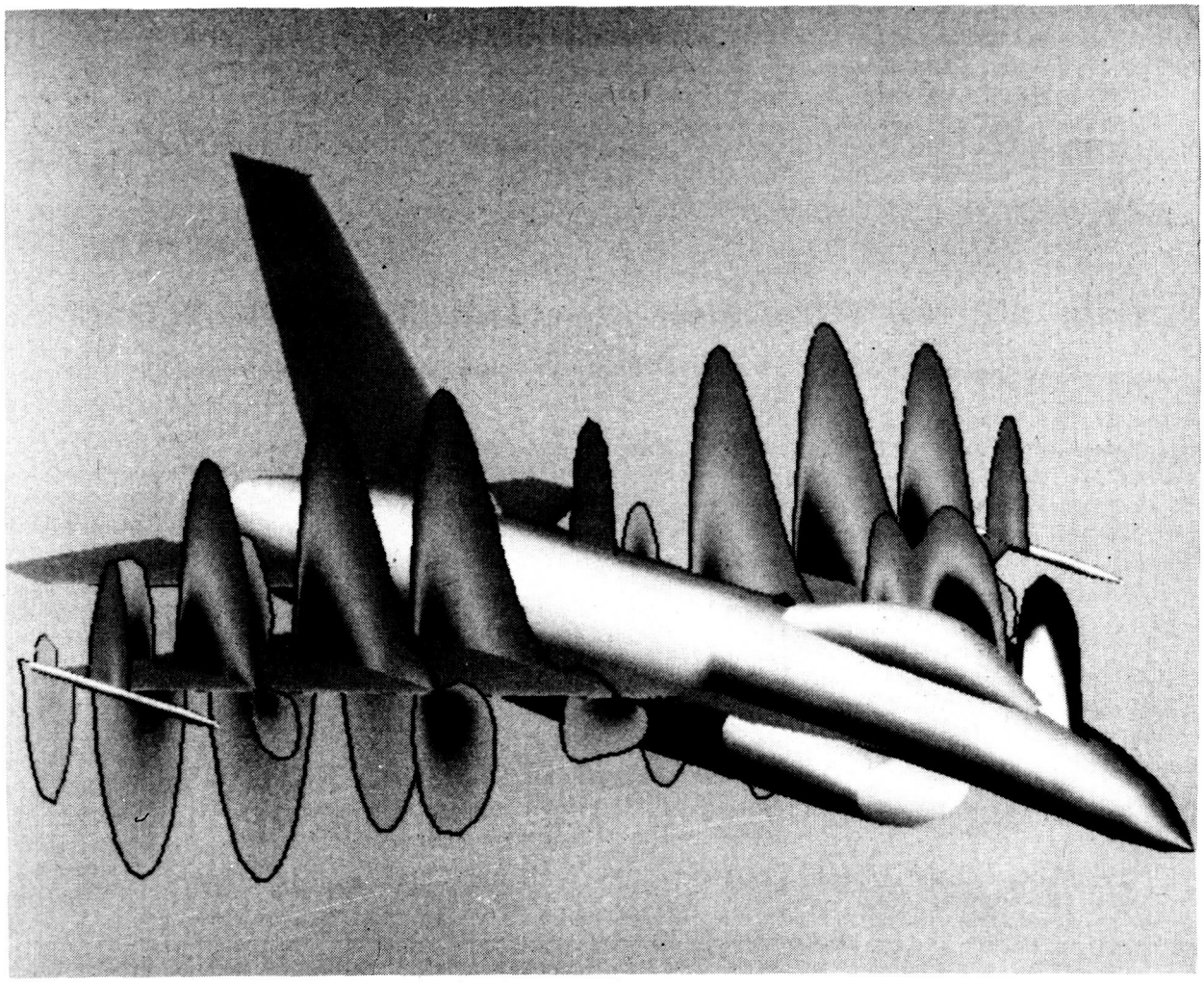

C-2

UNSTEADY FLOW FIELD PRESSURES FOR F-16C AIRCRAFT AT MAXIMUM PITCH ANGLE

Instantaneous flow field pressures at two points during a cycle of the rigid aircraft pitching calculations are shown in the next two figures. This figure shows contours at the aircraft maximum pitch angle; the next figure shows contours at the aircraft minimum pitch angle. The pressures shown here indicate an increase in the overall levels of both compression and expansion as the aircraft pitches up.

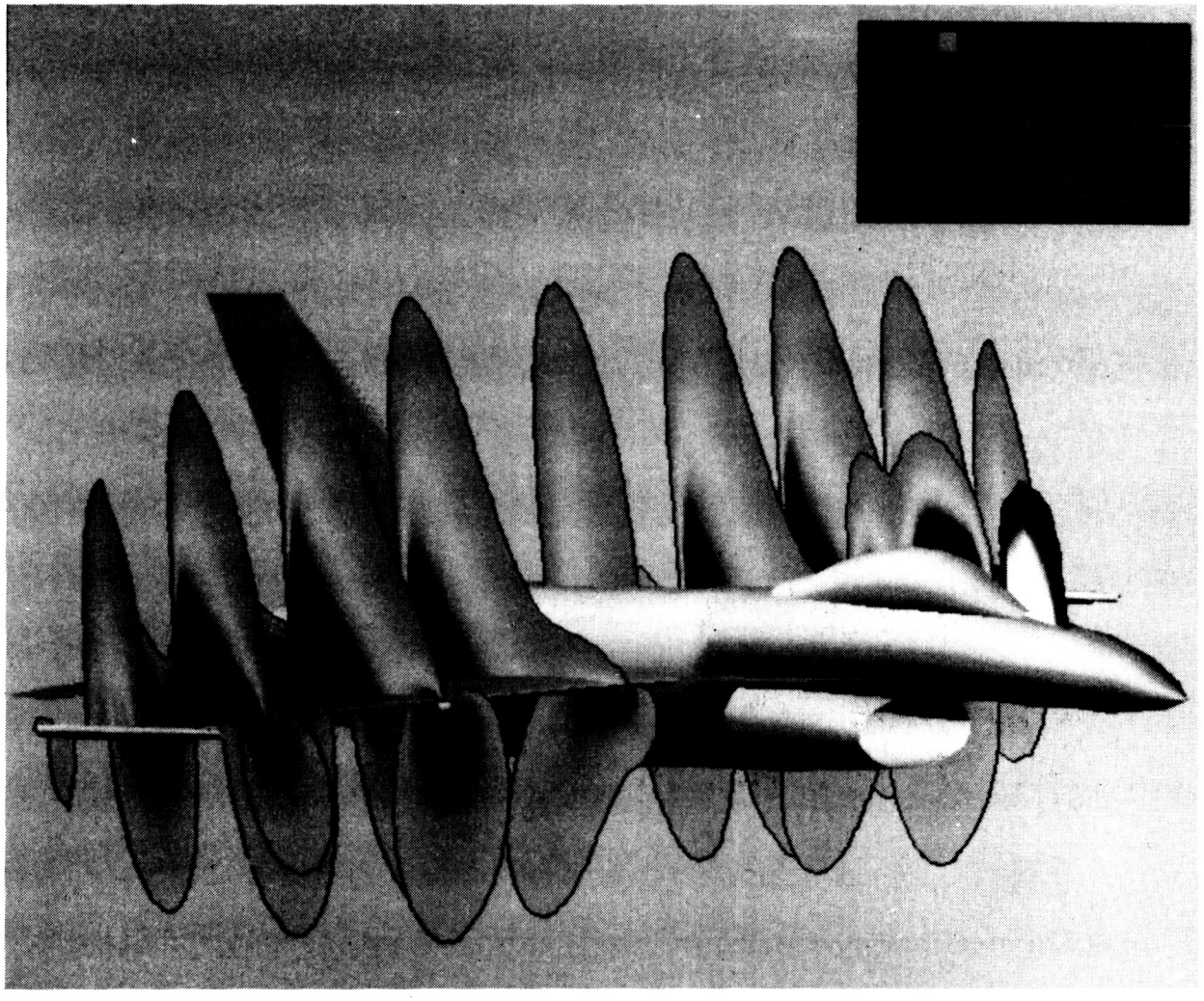

UNSTEADY FLOW FIELD PRESSURES FOR F-16C AIRCRAFT AT MINIMUM PITCH ANGLE

As the aircraft pitches down, the pressure levels decrease significantly along the wing, as shown in the figure.

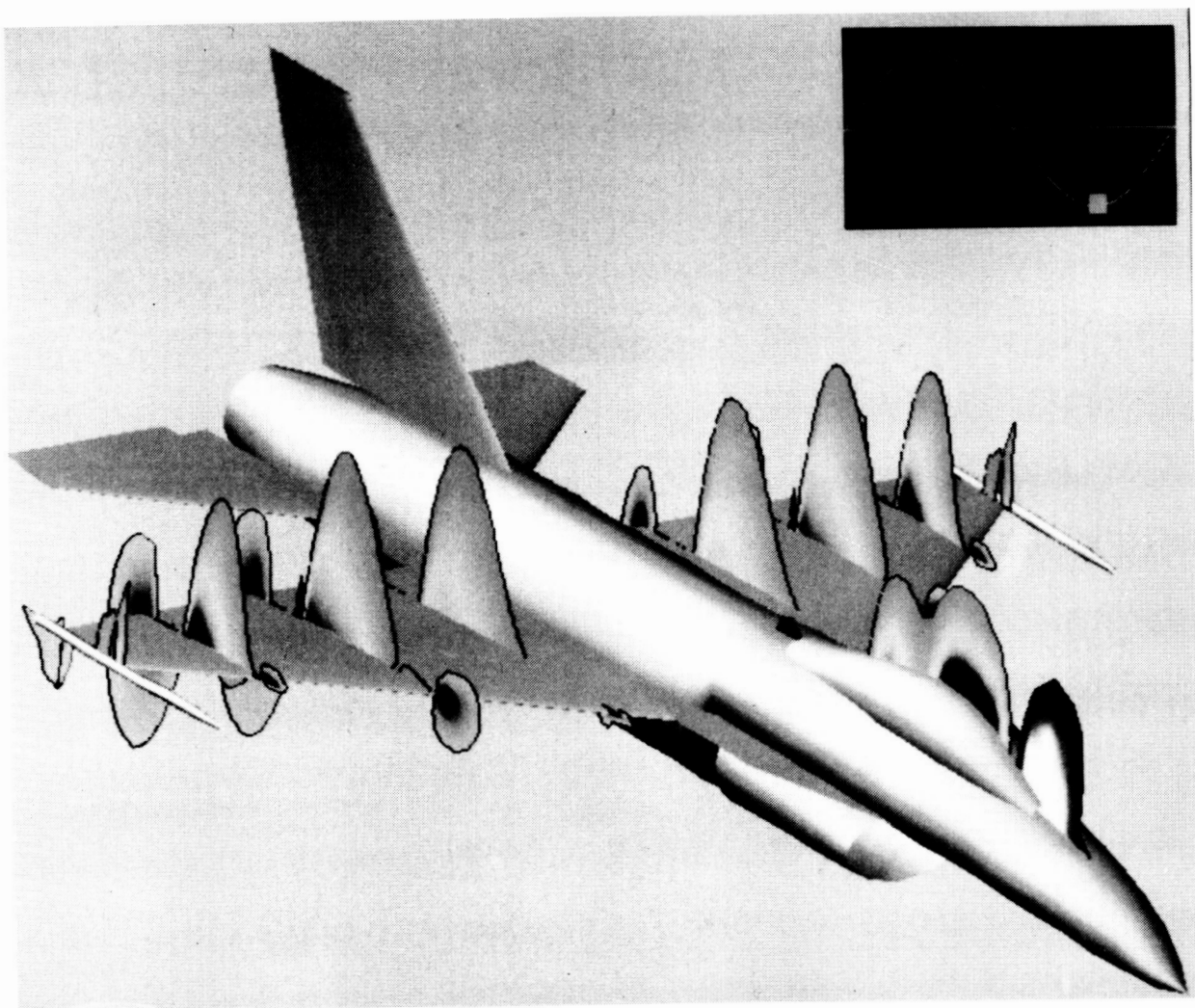

STEADY SURFACE PRESSURES FOR F-16C AIRCRAFT

The other view plotted is the planform view of the aircraft. Here the upper surface pressures are contoured similarly to the oblique projection results. This figure shows the steady surface pressures at M = 0.9 and $\alpha_0 = 2.38^0$. In this view, the shock wave is clearly represented by the lateral line on the wing near 75 - 80% chord. The shock is strongest outboard where there is a rapid change in contour level.

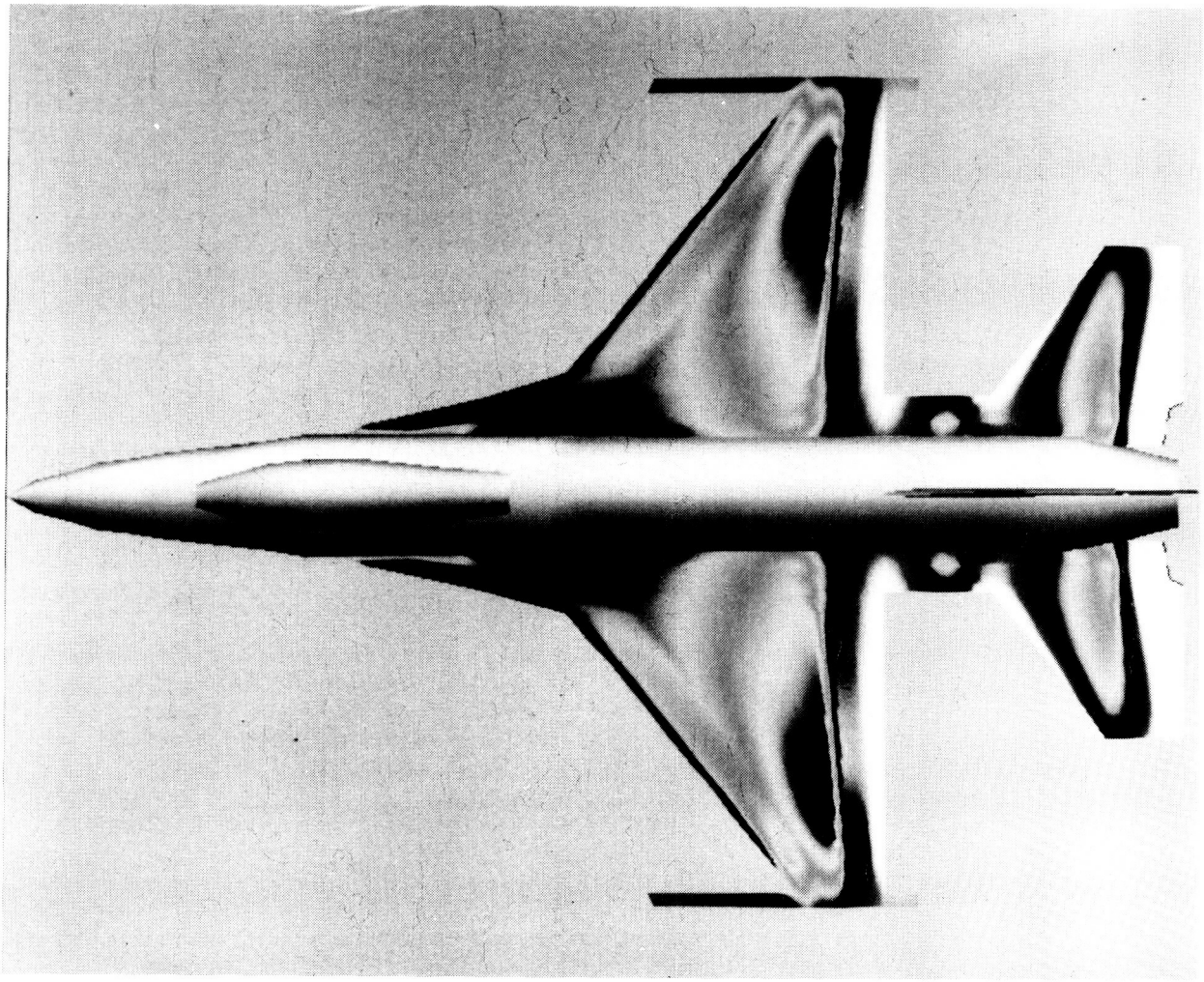

UNSTEADY SURFACE PRESSURES FOR F-16C AIRCRAFT AT MAXIMUM PITCH ANGLE

Instantaneous pressures at two points during the cycle of rigid aircraft pitching are shown in the next two figures. Near the aircraft maximum pitch angle (shown here) the embedded supersonic region becomes larger as indicated by the increased size of the black contouring on the upper surface of the wing. Also, the shock becomes relatively strong as indicated by the rapid change in contour level, from black to white.

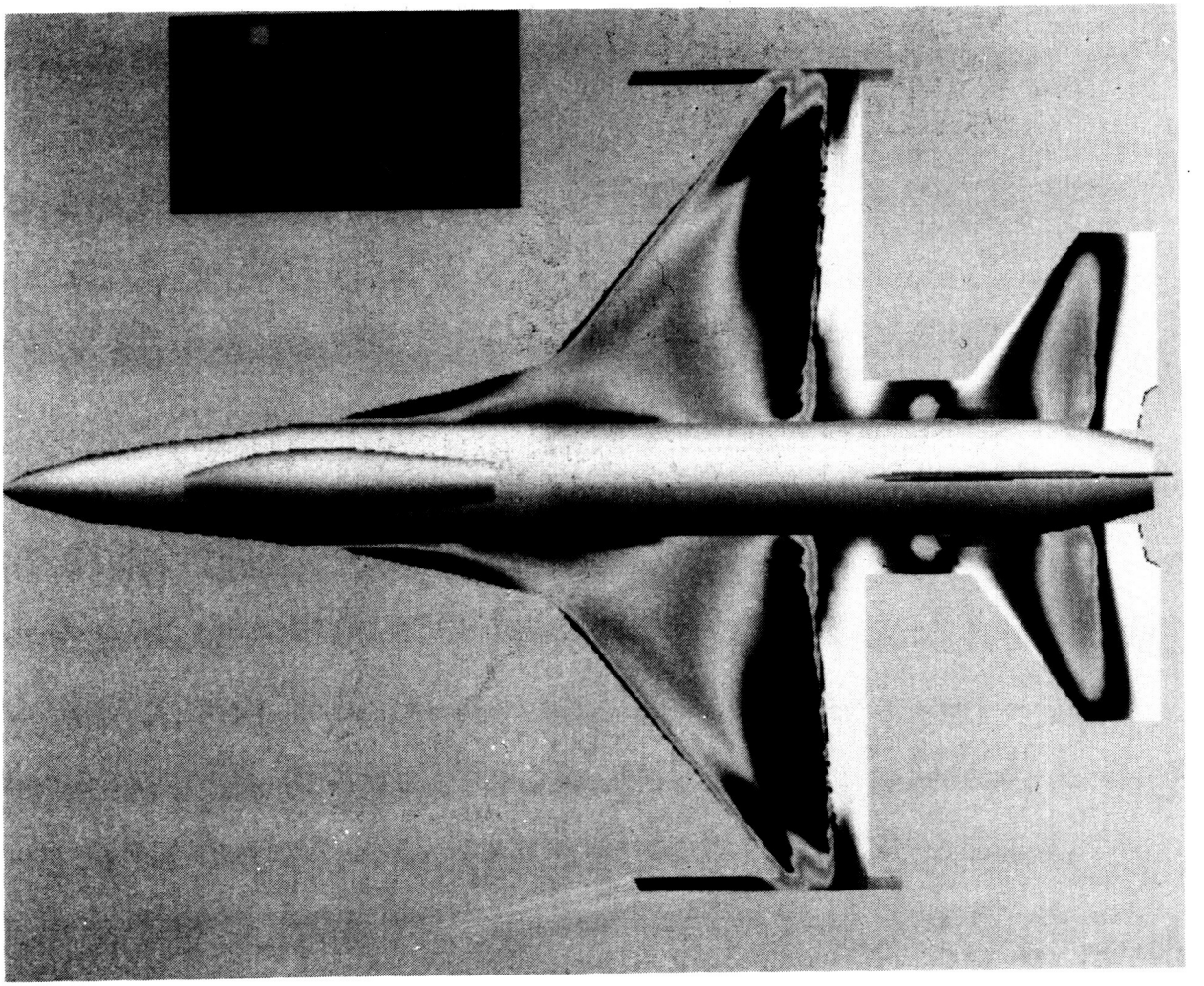

UNSTEADY SURFACE PRESSURES FOR F-16C AIRCRAFT AT MINIMUM PITCH ANGLE

Near the aircraft minimum pitch angle, shown in this figure, the shock on the wing upper surface becomes relatively weak and the flow is more compressed in the inboard region along the strake.

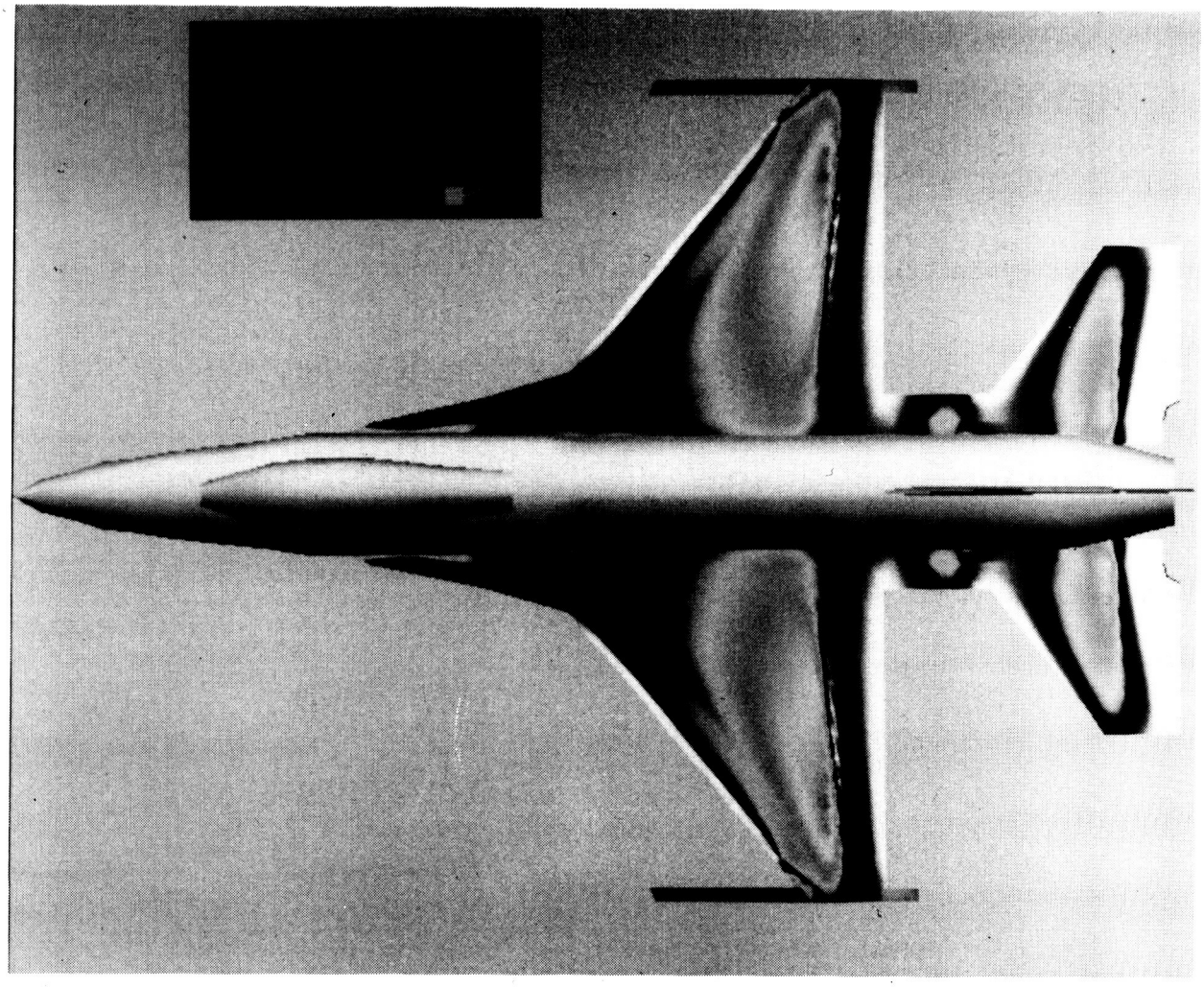

CONCLUDING REMARKS

A transonic unsteady aerodynamic and aeroelasticity code called CAP-TSD has been developed for application to realistic aircraft configurations. The name CAP-TSD is an acronym for Computational Aeroelasticity Program - Transonic Small Disturbance. The new code now permits the calculation of unsteady flows about complete aircraft configurations for aeroelastic analysis in the flutter critical transonic speed range. The CAP-TSD code uses a time-accurate approximate factorization (AF) algorithm for solution of the unsteady transonic small-disturbance equation. The AF algorithm has been shown to be very efficient for steady or unsteady transonic flow problems. It can provide accurate solutions in only several hundred time steps yielding a significant computational cost savings when compared to alternative methods. For reasons of practicality and affordability, an efficient algorithm and a fast computer code are requirements for realistic aircraft applications.

Results were presented for several complex aircraft configurations which demonstrated the geometrical applicability of CAP-TSD. The code can treat configurations with arbitrary combinations of lifting surfaces and bodies including canard, wing, tail, control surfaces, tip launchers, pylons, fuselage, stores, and nacelles. These calculated results were in good agreement with the experimental pressure data which assessed CAP-TSD for multiple components applications with mutual interference effects.

Finally, results were presented for the General Dynamics one-ninth scale F-16C aircraft model which demonstrated application to a realistic configuration. Steady results compared well with the experimental data. Unsteady results for the entire F-16C aircraft undergoing a rigid pitching motion were presented. Comparisons with parallel wing alone results revealed aerodynamic interference effects of the additional aircraft components on wing unsteady pressures. These effects emphasize the importance of including all components in the calculation. The CAP-TSD code thus provides the capability of modeling complete aircraft configurations for realistic transonic unsteady aerodynamic and aeroelastic analyses. Further pressure correlations and aeroelastic calculations are presently underway to continue assessing and validating the code.

- CAP-TSD code models complete aircraft configurations for transonic unsteady aerodynamic and aeroelastic analyses
- Initial pressure comparisons show good agreement
- Further pressure correlations and aeroelastic calculations presently underway to continue validating code

REFERENCES

[1]Batina, J. T.: "An Efficient Algorithm for Solution of the Unsteady Transonic Small-Disturbance Equation," AIAA Paper No. 87-0109, Presented at the AIAA 25th Aerospace Sciences Meeting, Reno, Nevada, January 12-15, 1987. (Also available as NASA TM 89014, December 1986).

[2]Batina, J. T.; Seidel, D. A.; Bland, S. R.; and Bennett, R. M.: "Unsteady Transonic Flow Calculations for Realistic Aircraft Configurations," AIAA Paper No. 87-0850, Presented at the AIAA/ASME/ASCE/AHS 28th Structures, Structural Dynamics, and Materials Conference, Monterey, California, April 6-8, 1987. (Also available as NASA TM 89120, March 1987).

[3]Persoon, A. J.; Roos, R.; and Schippers, P.: "Transonic and Low Supersonic Wind-Tunnel Tests on a Wing with Inboard Control Surface," AFWAL-TR-80-3146, December 1980.

[4]Renirie, L.: "Analysis of Measured Aerodynamic Loads on an Oscillating Wing-Store Combination in Subsonic Flow," NLR MP 74026 U, September 1974.

[5]Bennekers, B.; Roos, R.; and Zwaan, R. J.: "Calculation of Aerodynamic Loads on Oscillating Wing/Store Combinations in Subsonic Flow," NLR MP 74028 U, September 1974.

[6]Korner, H.; and Schroder, W.: "Druckverteilungs- und Kraftmessungen an einer Flugel-Rumpf-Leitwerk-Anordnung," DFVLR-IB-080-72/13, 1972.

[7]Stewart, V. R.: "Evaluation of a Propulsive Wing/Canard Concept at Subsonic and Supersonic Speeds," Rockwell International Report NR82H-85, February 1983.

[8]Fox, M. C.; and Feldman, C. S.: "Model and Test Information Report, 1/9-Scale F-16C and F-16D Force and Loads Model," General Dynamics Report 16PR2179, January 1982.

[9]Feldman, C. S.: "Wind Tunnel Data Report, 1/9-Scale F-16C Pressure Loads Test," General Dynamics Report 16PR2252, July 1982.

[10]Bennett, R. M.; Bland, S. R.; Batina, J. T.; Gibbons, M. D.; and Mabey, D. G.: "Calculation of Steady and Unsteady Pressures on Wings at Supersonic Speeds with a Transonic Small-Disturbance Code," AIAA Paper No. 87-0851, Presented at the AIAA/ASME/ASCE/AHS 28th Structures, Structural Dynamics, and Materials Conference, Monterey, CA, April 6-8, 1987.

[11]Gibbons, M. D.; Whitlow, W., Jr.; and Williams, M. H.: "Nonisentropic Unsteady Three Dimensional Small Disturbance Potential Theory," AIAA Paper No. 86-0863, Presented at the AIAA/ASME/ASCE/AHS 27th Structures, Structural Dynamics, and Materials Conference, San Antonio, Texas, May 19-21, 1986.

[12]Howlett, J. T.: "Efficient Self-Consistent Viscous-Inviscid Solutions for Unsteady Transonic Flow," AIAA Paper No. 85-0482, Presented at the AIAA 23rd Aerospace Sciences Meeting, Reno, Nevada, January 14-17, 1985.